Simulation of the hydrodynamics in the onset of fouling for oil-water core-annular flow in a horizontal pipe

Jiang, Fan; Li, Haoyu; Pourquié, Mathieu; Ooms, Gijs; Henkes, Ruud

DOI
10.1016/j.petrol.2021.109084

Publication date
2021

Document Version
Final published version

Published in
Journal of Petroleum Science and Engineering

Journal of Petroleum Science and Engineering 207 (2021) 109084

Contents lists available at ScienceDirect

Journal of Petroleum Science and Engineering

journal homepage: www.elsevier.com/locate/petrol

Simulation of the hydrodynamics in the onset of fouling for oil-water core-annular flow in a horizontal pipe

Fan Jiang [a,b], Haoyu Li [b], Mathieu Pourquié [b], Gijs Ooms [b], Ruud Henkes [b,*]

[a] School of Mechanical and Electric Engineering, Guangzhou University, Guangzhou, 510006, China
[b] J.M. Burgers Centre for Fluid Mechanics, Delft University of Technology, Faculty of Mechanical, Maritime, and Materials Engineering (3mE), Laboratory for Aero- & Hydrodynamics, Mekelweg 2, 2628, SC, Delft, the Netherlands

ARTICLE INFO

Keywords:
Core-annular flow
Pipeline transport
Fouling hydrodynamics
CFD simulation

ABSTRACT

Core-annular flow is an efficient way of transporting viscous oil through a pipeline. A sharp increase in the pressure drop will occur when the oil waves at the water-oil interface touch the pipe wall. Depending on the oil and pipe material physical properties, the oil may adhere to the wall leading to fouling. Therefore, a necessary requirement for the onset of oil fouling of the pipe wall is that the flow hydrodynamics allow the oil to reach and touch the wall. With respect to the problem statement, this study deals with finding the hydrodynamic conditions under which core-annular flow becomes unstable and the oil waves touch the pipe wall. The method that is followed is to resolve the first-principle set of equations that describe the hydrodynamics: the Reynolds-Averaged Navier-Stokes (RANS) equations are solved using Computational Fluid Dynamics (CFD) in the opensource package OpenFOAM. Simulations were carried out for the horizontal pipe with two diameters (10.5 and 21 mm), at a range of imposed pressure drops and water holdup fractions (giving the mixture velocity and watercut as output). Most simulations were carried out for an oil to water viscosity ratio of 1040 (but also a variation of this was considered). For each value of the pressure drop (or mixture velocity) there is a critical value of the watercut below which the oil reaches the pipe wall. This critical value of the watercut is lower for the larger pipe diameter of 21 mm, namely about 9.6%, than for the smaller pipe diameter of 10.5 mm, namely about 14% (for a viscosity ratio $m = 1040$). Wall touching occurs when the mixture velocity is too low, but this lower limit is significantly higher for the larger pipe diameter of 21 mm, namely about 1.1 m/s, than for the smaller pipe diameter, namely about 0.3 m/s (for a viscosity ratio $m = 1040$). The main conclusion is that a state-of-art CFD approach is capable of simulating the growth of waves at the oil-water interface until they touch the pipe wall, which is a necessary condition for the onset of fouling.

1. Introduction

Oil-water core-annular flow can lead to energy saving for transporting viscous oil (also referred to as heavy oil) through a pipeline. In this flow regime a water layer lubricates the full perimeter of the pipe wall, which sharply reduces the pressure drop and herewith the required pump capacity. Because of its practical application and because of the remarkable underlying fluid mechanics, this technology of water-lubricated transport of crude oil has been studied extensively for decades (Ooms, 1972; Arney et al., 1996).

For example, Oliemans and Ooms (1986) reviewed the theoretical models and correlation methods of oil-water core-annular flow in a pipeline. Joseph et al. (1997) gave an overview of oil-water core-annular flow, which included stability, industrial experience, measures of energy efficiency, and models of levitation. Ghosh et al. (2009) also provided a review on oil-water core-annular flows, which included pressure drop reduction, stability, and wettability. Also experimental studies have been reported for oil-water core-annular flow. For instance, Rodriguez and Bannwart (2006) conducted an experimental study on interfacial waves and the holdup in oil-water core-annular flow and provided a flow pattern map for the appropriate design of the heavy oils transportation system. Also Sotgia et al. (2008) performed an experimental analysis for the flow regime and pressure drop in oil-water flow, and the results were used to determine the required operational conditions for core-annular flow. Jing et al. (2016) experimentally studied the heavy oil and water flow behaviour for different temperatures (giving different

* Corresponding author.
E-mail address: r.a.w.m.henkes@tudelft.nl (R. Henkes).

https://doi.org/10.1016/j.petrol.2021.109084
Received 8 February 2021; Received in revised form 7 June 2021; Accepted 8 June 2021
Available online 17 June 2021

oil viscosities). Van Duin et al. (2019) conducted an experimental investigation of oil-water core-annular flow in a horizontal pipe, and discussed the influence of the oil viscosity on the pressure drop.

Meanwhile, several theories have been proposed. Ooms et al. (1984) applied the lubrication theory to study core-annular flow in a horizontal pipe. Huang and Joseph (1995) investigated the linear stability of core-annular flow using the finite element method to solve the governing fluid dynamics equations. Bannwart (2001) developed phenomenological models for predicting the holdup and pressure drop for horizontal and vertical core-annular flow. Ooms et al. (2013) analysed the counter-balance behaviour of the buoyancy force on the oil core under different wave forms.

Many simulation studies have been performed as well. Ooms et al. (2013) made a numerical study to investigate the buoyancy force on the oil core in horizontal core-annular flow. Beerens et al. (2014) used the volume of fluid method to simulate core-annular flow, and the simulation results showed a satisfactory agreement with theoretical results and experimental data. Ingen Housz et al. (2017) performed an experimental and numerical study for horizontal oil-water core-annular flow. They analysed the effect of the presence of turbulence in the water annulus, and the simulated results agreed well with the experimental data.

It is evident that oil-water core-annular flow can be an attractive industrial approach, as it significantly reduces the frictional pressure drop. However, as soon as the oil wets the pipe wall a sharp increase in pressure drop occurs and this will prohibit the proper oil transport. Arney et al. (1996) experimentally observed that the oil would easily foul a carbon steel pipe wall, whereas the use of a cement-lined pipe could prevent fouling. Joseph et al. (1999) found that the oil will easily foul the pipe wall when a too small volume of water is used. Bannwart (2001) observed the oil fouling process in a steel tube, and found an increase in the pressure drop with fouling. McKibben et al. (2000) reported the same. Also Vuong et al. (2009) detected how the oil core was sticking to the pipe wall in their experiment. Sridhar et al. (2011) found in their experiments that the oil fouling of the wall is probably related to the wettability of the pipe wall. Ghosh et al. (2011) reported simulations of core-annular flow through a bend, and they formulated operating conditions to avoid the fouling. Kaushik et al. (2012) observed that fouling occurred downstream of the expansion in both the experiments and simulations of core-annular flow through such an expansion, and operating conditions were found to avoid the fouling. Ooms et al. (2013) simulated the core-annular flow in a horizontal pipe without inertial terms in the motion equations, and found how the oil core continued to move upward until it touched the pipe wall. Jiang et al. (2014) simulated the oil-water core-annular flow through a return bend, and discussed the fouling behaviour. Shi et al. (2017a,b) simulated the water holdup and the pressure gradient of core-annular flow in horizontal pipes, and considered the impact of oil fouling on the pressure gradient.

In their overview of core-annular flow, Joseph et al. (1997) distinguish four flow regimes of water-lubricated oil flow: (i) perfect core-annular flow, (ii) wavy core-annular flow, (iii) slugs of oil in water, and (iv) drops of oil in water. Depending on the conditions, these states can be hydrodynamically stable. However, lubrication may fail due to: (i) fouling, (ii) transition to stratification under gravity when the density difference is large (and the core velocity is too low to levitate the core off the wall), and (iii) inversion to water in oil emulsions. Furthermore, Joseph et al. (1997) mention that failure due to stratification at low speeds is characteristic for large diameter pipes in which capillary forces are not important. In small pipes, slugs of oil separated by water will stratify in the pipe.

More recently, a few studies that use Computational Fluid Dynamics (CFD) for core-annular flow with a turbulent water annulus have appeared. These include the Reynolds-Averaged Navier Stokes (RANS) results for a horizontal pipe by Archibong-Eso et al. (2019) and Direct Numerical Simulations (DNS) for a vertical pipe by Kim and Choi (2018).

In an effort to expand the knowledge on the onset of wall fouling by the oil core in core-annular flow, detailed simulations were carried out in the present study. Here the focus is fully on the hydrodynamics that can lead to the case that the oil touches the pipe wall. This is a necessary requirement for the onset of fouling. Thereto the Navier-Stokes equations were solved using the open-source CFD package OpenFOAM, using a low-Reynolds number k-ε model for the turbulent water annulus. The wave formation at the oil-water interface is monitored. In a systematic way, the onset is determined for a horizontal pipe with two different diameters. The simulation results are used to construct the wall-touching line, which describes the critical watercut below which the oil can reach the pipe wall, as a function of the mixture velocity.

We have used the state-of-the art OpenFOAM tool in this study. This is an open-source general-purpose package for single phase and multiphase Computational Fluid Dynamics. As far as the authors know this is the first time that a CFD method is used to get some systematic insight in the fluid flow aspects of the unstable growth of waves at the oil-water interface in horizontal core-annular flow to the extent that the oil waves grow to touch the pipe wall. Whether the oil sticks and fouls the wall depends on the precise constituents of the oil and its physical properties as well as of the material properties of the pipe wall. For the fouling different correlations exist in the literature. However, the fluid dynamics need to allow the oil to reach the wall before fouling can occur. The novelty of our study lies in the application of a first-principles prediction method for the flow structure of core-annular flow (with a viscous oil core and a turbulent water annulus) and the possible tendency of the oil to touch the pipe wall. This can be combined with a fouling correlation to determine whether the oil that has touched upon the wall will stick to it to give fouling.

2. Mathematical model

2.1. Governing equations

The governing equations of the incompressible, isothermal flow are the conservation laws of mass and momentum, which can be written as follows:

$$\nabla \cdot \vec{u} = 0 \tag{1}$$

$$\frac{\partial(\rho\vec{u})}{\partial t} + \nabla\cdot(\rho\vec{u}\vec{u}) = -\nabla p + \nabla\cdot\mu(\nabla\vec{u} + \nabla\vec{u}^T) + \rho\vec{g} + \vec{F}_\sigma \tag{2}$$

Where $\vec{u}$ is the velocity vector, ρ is the fluid density, μ is the fluid viscosity, g is the gravitational acceleration, p is the pressure and $\vec{F}_\sigma$ is the interfacial tension force.

2.2. VOF (Volume of fluid) method

The VOF method uses a marker function α which satisfies the following conservation equation (Yamamoto et al., 2017):

$$\frac{\partial\alpha}{\partial t} + \vec{u}\cdot\nabla\alpha = 0 \tag{3}$$

Here the marker function α is described as the volume fraction of oil and water as

$$\alpha = \begin{cases} 0 & \text{water} \\ 1 & \text{oil} \\ 0 < \alpha < 1 & \text{interface} \end{cases} \tag{4}$$

The density ρ and viscosity μ in eq. (2) are described by using the oil volume fraction α_o and the water volume fraction α_w as

$$\rho = \alpha_o\rho_o + \alpha_w\rho_w \tag{5}$$

$$\mu = \alpha_o\mu_o + \alpha_w\mu_w \tag{6}$$

Here ρ_w is the water density, ρ_o is oil density, μ_w is the water viscosity, and μ_o is the oil viscosity. Furthermore, $\alpha_o = \alpha$ is the volume fraction of oil, while $\alpha_w = (1-\alpha)$ is the volume fraction of water.

In eq. (2), the external force is the surface tension force, which is described by the continuum surface force (CSF) model.

2.3. Coupled VOF and Level Set method

In the Level Set method, the level function (φ) is related to the VOF (α) field in the following way (Yamamoto et al., 2017):

$$\varphi_0 = (2\alpha - 1)\Gamma \tag{7}$$

$$\frac{\partial \varphi}{\partial \tau} = \mathrm{sign}(\varphi_0)(1 - |\nabla\varphi|) \tag{8}$$

$$\varphi(x, 0) = \varphi_0(x) \tag{9}$$

Here Γ is a non-dimensional number with $\Gamma = 0.75\Delta x$, Δx is the grid spacing; $\Delta\tau$ is the artificial time step with $\Delta\tau = 0.1\Delta x$.

In the CLSVOF method, the CSF model based on the LS function can be described as

$$F_{\sigma,\varphi} = \sigma_{ow} k_\varphi \delta_\varphi \nabla\varphi \tag{10}$$

in which the delta function δ_φ is expressed as

$$\delta_\varphi = \begin{cases} \frac{1}{2e}\left(1 + \cos\left(\frac{\pi\varphi}{e}\right)\right) & |\varphi| < e \\ 0 & \text{elsewhere} \end{cases} \tag{11}$$

Where e is the interface thickness with $e = 1.5\Delta x$.

3. Numerical solution

3.1. Geometry

The flow domain is a pipe section with radius $R_2 = D/2$, which is the same as in the experimental pipe used by our group. The diameter is set to 21 mm (same as in the experimental pipe used by our group) or to half that value. The length L of the pipe section in the simulations is 25.6 mm, which is about double the length of the fastest growing interface waves (as found in the lab experiments).

3.2. Meshing of the flow domain

The geometry is meshed by a combination of block-structured and unstructured grids with 125, 80, and 60 cells in radial, circumferential and axial flow direction, respectively. This gives a total of about 230,000 grid cells. As shown in Fig. 1, the grid is finer near the pipe wall than at the pipe centre in order to properly capture the wall approach process.

3.3. Solution strategy

The CFD package OpenFOAM version 2.1.1 was used for these simulations. The numerical discretisation scheme is: backward Euler in time, the limited linear scheme for the advection of the interface, the Van Leer scheme for the advection of the velocity, and the first-order upwind scheme for the advection of the turbulent properties k and ε. The algorithm employed the CLSVOF model of Yamamoto et al. (2017) to obtain a sharp interface. The pressure-velocity coupling was conducted by the PISO scheme. The following linear solvers have been used: Geometric Agglomerated Algebraic Multigrid for the pressure and Preconditioned Bi-Conjugate Gradient for velocity components. The turbulence of the water annulus was covered by the Launder-Sharma low-Reynolds number k-ε model (Reynolds-Averaged Navier-Stokes approach, RANS). The Courant number was set to 0.01.

3.4. Fluid properties and boundary conditions

The thermodynamic properties of water and oil in field applications will depend on the temperature (and to a lesser degree also on the on the pressure). In particular, a decrease/increase in temperature will increase/decrease the oil viscosity. In this simulation study we have assumed isothermal conditions (i.e. the energy equation, with heat transfer was not included). However, we did consider the effect of a variation in oil viscosity. In each simulation the value of the oil viscosity was imposed (whereas in field operation such a variation could be caused by the temperature change). Only the viscosity, density, and surface tension were considered; other specific features of the water and oil combination, such as emulsion tendency, were not considered.

The dynamic viscosities of the liquids in the core and annulus are set to $\mu_o = 0.697$ Pa s and $\mu_w = 0.00067$ Pa s, the densities are $\rho_o = 902$ kg/m^3 and $\rho_w = 993$ kg/m^3, and the interfacial tension is $\sigma = 0.016$ N/m.

Periodic boundary conditions were applied in axial direction. The pressure drop was imposed as a body force, which remained the same during a simulation. In addition the water holdup fraction was imposed at the start of a simulation, which was conserved during the simulation, thanks to the VoF method. At the pipe wall, the no-slip, no penetration boundary condition was prescribed (Beerens et al., 2014; Ingen Housz et al., 2017).

The time dependent, three dimensional CFD model only considers a local short pipe section (of 26 mm in length) with a constant pressure gradient. As mentioned, periodic boundary conditions are applied at the inlet and outlet of a pipe section. By doing this, a local fully developed flow has been assumed, which means that the flow is not dependent on the pipe inflow or on the upstream pipe flow development. Note that this local approach has an analogy with engineering 1D pipeline simulations, in which usually local flow equilibrium is assumed which can be solved by a single-point model. In the present study such a single-point model thus consists of a time-dependent 3D CFD model.

As the initial condition, perfect laminar core-annular flow was

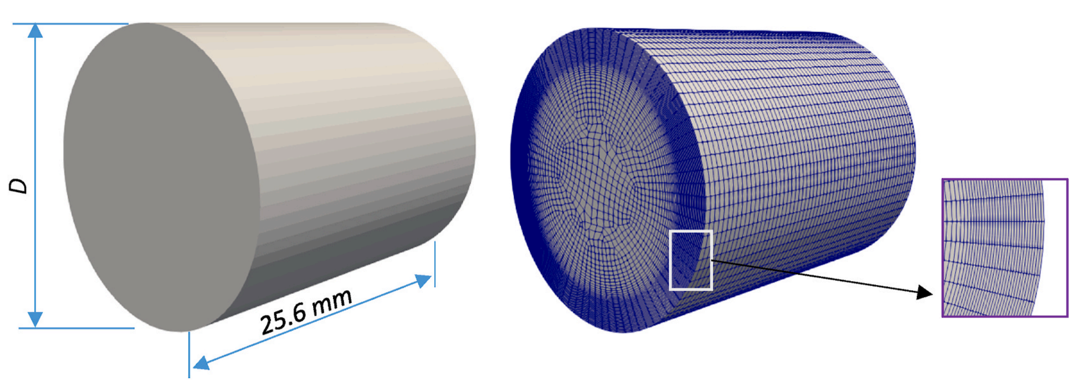

Fig. 1. Configuration with numerical grid.

assumed, for which an analytical solution exists for the streamwise velocity:

$$U_z = \begin{cases} U_c\left(1 - \frac{1}{m}r^{*2}\Big/A\right) & 0 < r^* < 1 \\ U_c\left(a^2 - r^{*2}\right)/A & r^* \geq 1 \end{cases} \tag{12}$$

Where U_c is initial centre line velocity, which was set to 1.245 m/s. In this expression $A = \frac{1}{m} + a^2 - 1$; $r^* = r/R_1$ (in which r is the local radius, i.e. $r = \sqrt{x^2 + y^2}$; $a = R_2/R_1$ (with R_1 being the pipe radius and R_2 being the radius of the oil core), and $m = \mu_o/\mu_w$.

In dimensionless form the oil flow rate Q_o and the water flow rate Q_w can be represented by the watercut ε_w and the mixture Reynolds number Re_m. These are defined as:

$$\varepsilon_w = Q_w/Q_T \tag{13}$$

and

$$Re_m = \rho_m U_m D/\mu_m \tag{14}$$

respectively. Here $Q_T = Q_o + Q_w$ is the total volumetric flow rate and $U_m = Q_T/A$ is the mixture velocity, in which A is the cross-sectional area of the pipe. Furthermore, ρ_m and μ_m are the mixture density and the mixture dynamic viscosity, which are defined as:

$$\rho_m = \varepsilon_w\rho_w + (1 - \varepsilon_w)\rho_o \tag{15}$$

$$\mu_m = \varepsilon_w\mu_w + (1 - \varepsilon_w)\mu_o \tag{16}$$

4. Results

In order to validate the simulations, experimental results obtained in our team for the horizontal pipe with 21 mm diameter were used. Both conditions without and with wall touch of the oil were measured; see the pictures from the experiments in Fig. 2 (Van Duin, 2017; Radhakrishnan, 2016). The simulation results for the oil-water interface for the two experimental conditions are shown in Fig. 3. Comparing Figs. 2 and 3, there is good agreement between the simulations and the experiments.

4.1. The wall touch line

To study the near wall flow dynamics of core-annular flow in horizontal pipes, the movement of the oil-water interface over time is monitored in the simulations, starting from the condition with concentric core-annular flow. Fig. 4 shows the simulation results for a case in which the oil core continues to rise until it touches the upper pipe wall. As shown in Fig. 5, as soon as the oil touches the wall, the oil flow rate for the given pressure drop sharply decreases. As depicted in Fig. 6, the amplitude of the interface wave and the thickness of the water annulus are different for the cases without and with the oil touching the wall. When the oil reaches the wall, the thickness of the water annulus at the top sharply drops to zero, while the amplitude of the interface wave at the top increases.

To summarize, the near wall characteristics of unstable core-annular flow are as follows: 1) the oil core touches the pipe wall, 2) the oil flow rate decreases rapidly; 3) the water annulus at the top becomes thinner and the amplitude of the interface wave increases.

In the present work, the focus is on constructing the wall-touch line; that line marks the transition from conditions without and with oil reaching the pipe wall. By doing repeated simulations for different conditions, the wall-touch line can be found as follows. In a single simulation the pressure drop and the water holdup fraction are imposed. For a certain pressure drop repeated simulations are made for successively increased water holdup fractions. As a result we find the total flow rate (or the mixture velocity U_{mix}) and the watercut. The critical value of the watercut above which oil remains away from the wall and below which the oil reaches the wall gives a point on the wall-touch line. This is shown in Fig. 7. By repeating this for the different values of the pressure drop, the full wall-touch line (curve) can be constructed.

4.2. Dependence of the wall-touch line on different parameters

For the horizontal pipe with a diameter of 21 mm the pressure drop was varied between 900 Pa/m and 1500 Pa/m and the watercut was varied between 0.083 and 0.109. The results, with the interpolated wall-touch line, are depicted Fig. 8. It may be noted that the value of the watercut at the wall-touch line is almost independent of the pressure drop, and equal to about 0.092; however, a weak minimum seems to occur at a pressure drop of about 1200 Pa/m.

Fig. 9 shows the wall-touch line as function of the mixture velocity and the watercut. Thus for each value of the mixture velocity a point on the wall-touch line can be found, which is the critical value of the watercut below which the oil will touch the wall. Like for the dependence on the pressure drop, also for the mixture velocity a weak minimum for the watercut at the wall-touch line is found.

The oil viscosity is varied from 0.697 to 10 Pa s (as the water viscosity is kept the same, this corresponds to changing the viscosity ratio m is from about 1000 to 15,000). For a fixed pressure drop of 1100 Pa/m, the watercut was varied from 0.065 to 0.094, and the wall-touch line is shown in Fig. 10. The watercut at the wall-touch line shows a minimum at about $m = 7500$. Thus when the viscosity ratio is below 7500, the watercut at the wall-touch line increases with decreasing viscosity ratio. When the viscosity ratio is above 7500, the watercut at the wall-touch line slightly increases with increasing viscosity ratio.

In addition to the horizontal pipe with the diameter $D = 21$ mm, simulations were also carried out with a smaller pipe diameter of 10.5 mm, whereas all other conditions were kept the same (e.g. the oil viscosity was kept at 0.697 Pa s). Fig. 11 shows the relation between the critical watercut for the onset of oil reaching the pipe wall as function of the mixture velocity; the wall-touch line is compared for the two pipe diameters. This shows that a decrease of the pipe diameter moves the required watercut to prevent the oil from reaching the pipe wall (and thus to maintain core-annular flow) to a higher value. In addition a smaller pipe diameter also allows to prevent oil from reaching the pipe wall up to a lower value of the mixture velocity.

Fig. 12 gives two examples of the time evolution of the occurrence of

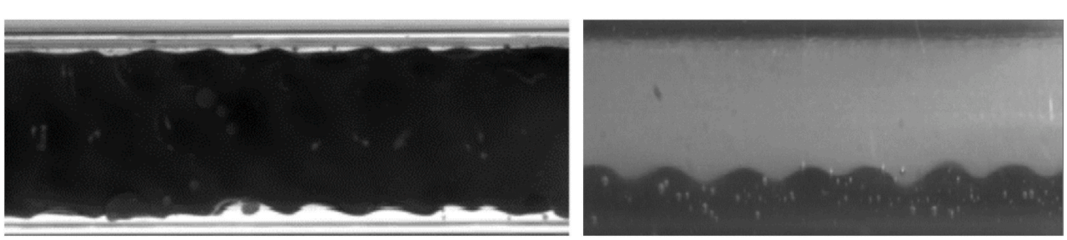

Fig. 2. Pictures from the flow experiments; (left) oil remains free from the wall (oil flow rate of 0.35 l/s and a watercut of 12%, oil density of 913 kg/m^3 and viscosity of 0.716 , Pa s Van Duin, 2017); (right) oil has reached the wall (oil flow rate of 0.146 l/s and a watercut of 12.5%, oil density of 857 kg/m^3 and a viscosity of 0.411 , Pa s Radhakrishnan, 2016). Note that the oil is black in the left graph and grey in the right graph.

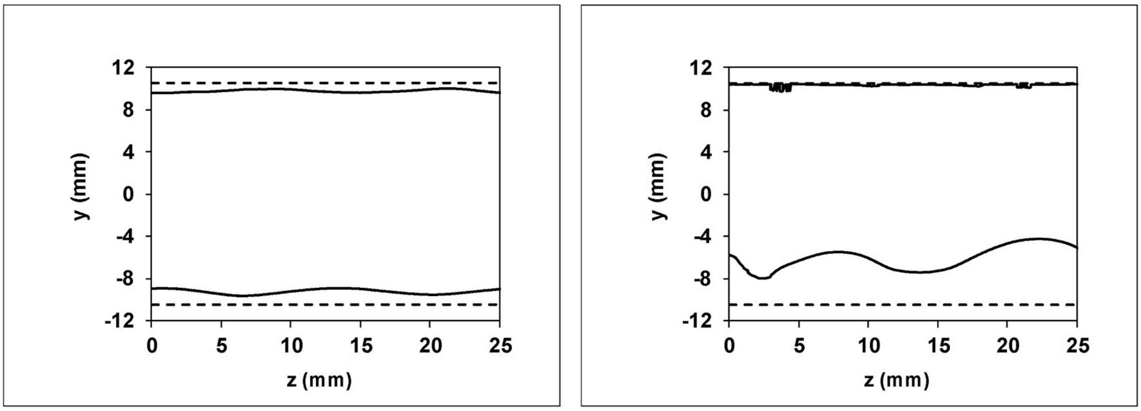

a) no oil at the wall b) oil at the wall

Fig. 3. The interface in the simulation results (dashed line is the wall, solid line is the interface).

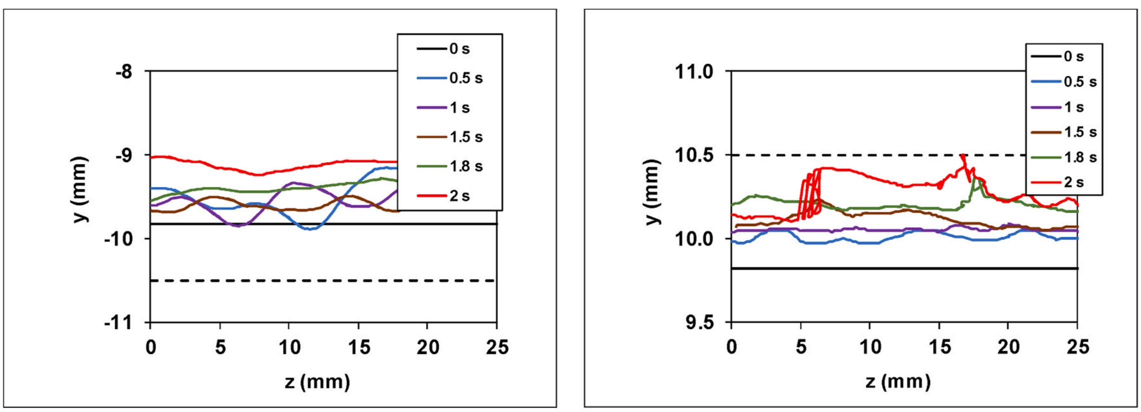

(a) Bottom interface (b) Top interface

Fig. 4. Temporal development of the interface at the bottom (left graph) and at the top (right graph) (D = 0.21 m, pressure drop is 1500 Pa/m, $\varepsilon_w = 0.0947$, m = 1040); dashed line denotes the wall location.

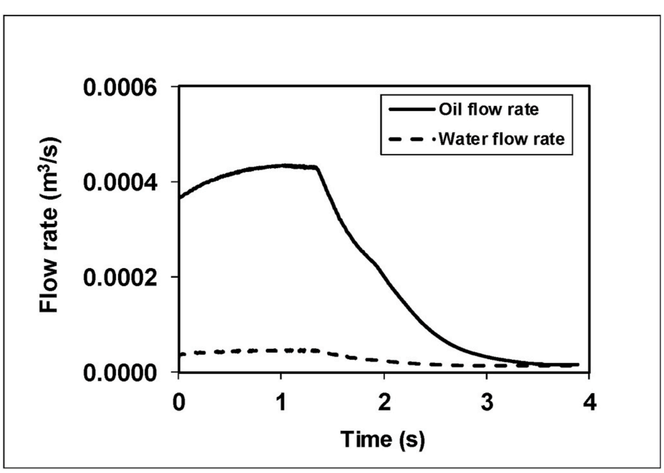

Fig. 5. Variation of the flow rates for the case with fouling (D = 0.21 m, pressure drop is 1500 Pa/m, ε_w = 0.0947, m = 1040).

oil reaching the pipe wall: one set of conditions for the 21 mm diameter pipe and one set of conditions for the 10.5 mm diameter pipe. Shown are the thickness of water annulus and the amplitude of the interface wave. The trends for the two cases are very similar. It can be noted that despite the difference in diameter by a factor 2, the thickness of the water annulus and the size of the amplitude of the interface waves is about the same for the two diameters. This shows that the absolute value of the water annulus and of the waves determine whether the oil can prevented or not to reach the pipe wall (and not their relative value with respect to the pipe diameter).

5. Discussion

In principle the water-oil flow through a horizontal pipe depends on the following 9 parameters: pipe diameter, oil and water flow rates, water and oil densities, water and oil viscosities, interfacial tension, and the gravitational acceleration. Using the Buckingham Π Theorem, the number of independent parameters can be reduced by three to give 6 dimensionless numbers. Clearly the dependence on these 6 dimensionless numbers of the flow regimes in a flow pattern map (and the proof of the stability of each flow regime) is very complex. Indeed it is quite ambitious to try solving the flow equations and draw conclusions on the occurrence and stability of the water lubricated flow regime. Nevertheless, in the present paper we have tried to demonstrate what can be achieved in this respect with a state of the art numerical flow solver.

In our transient simulations we started with perfect core-annular flow, and we monitored the interfacial wave formation and the upward movement of the oil core. When the oil touches the upper pipe wall, this can either be because core-annular flow cannot stably exist and there is transition to stratified flow (with water in the bottom layer

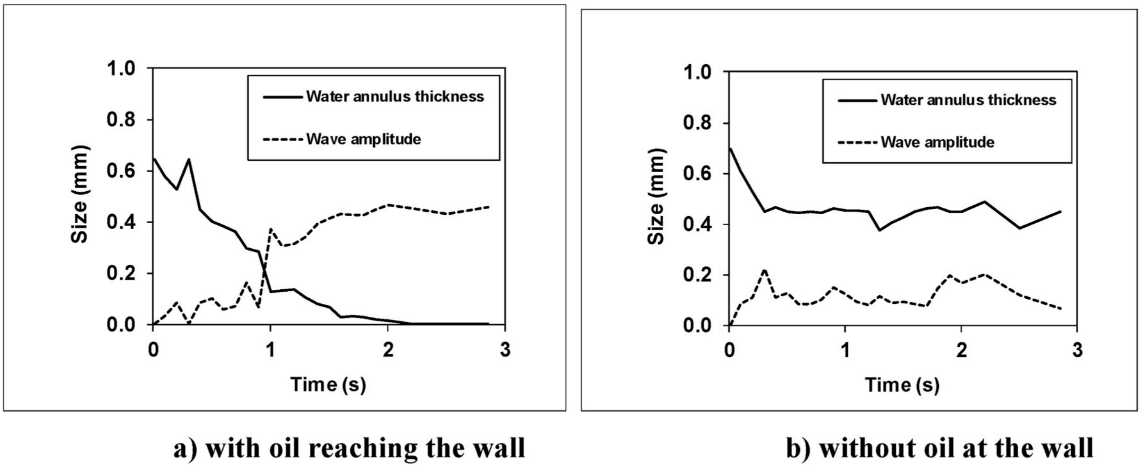

Fig. 6. The amplitude of the interface wave and the thickness of the water annulus for cases with and without the oil reaching the wall. $D = 0.21$ m and $m = 1040$; (a) pressure drop is 1200 Pa/m, $\varepsilon_w = 0.0896$, (b) pressure drop is 1100 Pa/m, $\varepsilon_w = 0.0965$.

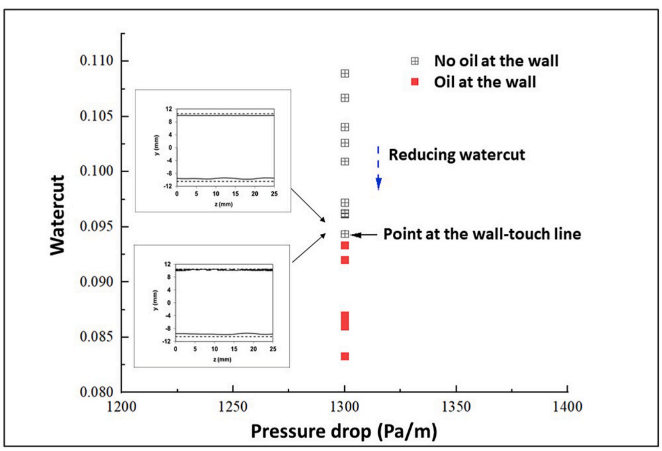

Fig. 7. Construction of the wall-touch line.

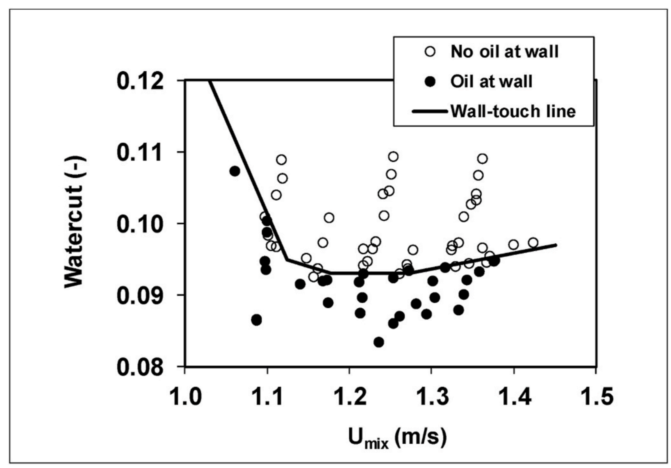

Fig. 9. The effect of the mixture velocity on the wall-touch line ($D = 21$ mm, $m = 1040$).

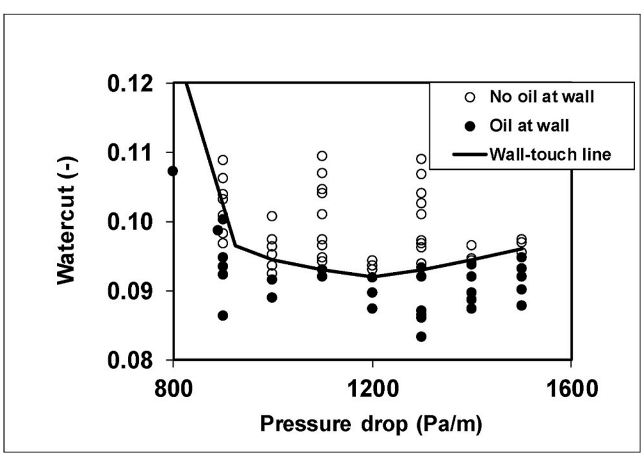

Fig. 8. The effect of the pressure drop on the wall-touch line ($D = 21$ mm, $m = 1040$).

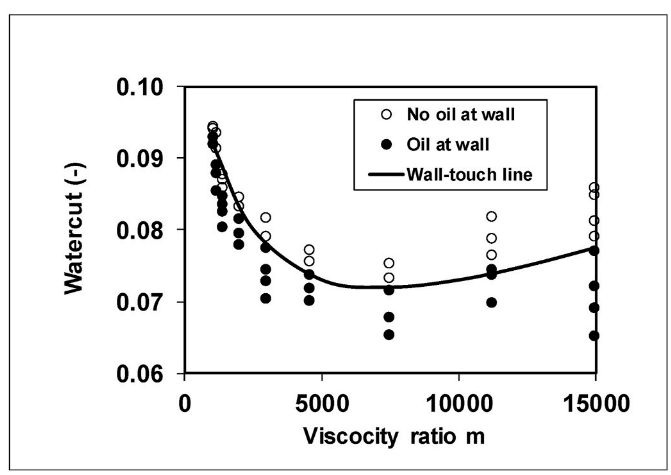

Fig. 10. The effect of the viscosity ratio on the wall-touch line for fixed pressure drop of 1100 Pa/m ($D = 21$ mm).

and oil the top layer) or the waves grow such large that they (temporarily or permanently) touch the wall. In actual reality for the latter condition, it depends on the adhesive properties between the oil and the pipe wall material whether the oil indeed remains stuck to the wall, and really fouls the wall. In the CFD simulations this adhesive behaviour is not explicitly modelled (in fact a default contact angle of 90 deg is used), and the simulation was stopped when the oil touched the pipe wall.

To further sketch the complexity of obtaining a full simulation-based

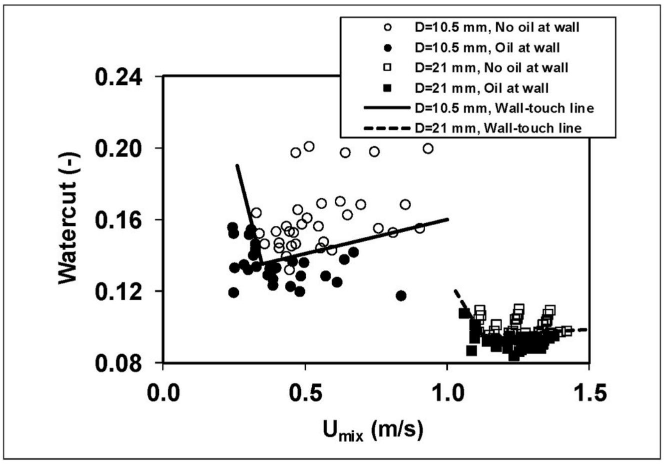

Fig. 11. The effect of the pipe diameter on the wall-touch line ($m = 1040$).

overview of the dependence of the wall touching process of the oil on the range of possible physical parameters the following can be considered. Each 3D simulation for a single set of conditions is very time consuming on the computer; each simulation takes a few days simulation time on the cluster computer that has been used in the present study. As mentioned, there are 6 dimensionless numbers that can play a role in the physics of the problem (and thus on the location of the wall-touch line). If each dimensionless number would be covered by say 10 values, a total of one million (10^6) conditions should be covered. In the present study we have only considered (for a relatively small selection of values) the dependence of fouling on the pipe diameter, on the mixture viscosity, and on the viscosity. In a future study it would of interest to also include the fouling dependence on the oi/water density ratio.

5.1. *Transition from core-annular flow to stratified flow*

Bannwart (2001) and Sotgia et al. (2008) have carried out experiments for various pipe diameters to determine the transition criteria for core-annular flow to stratified flow. The first criterion, as proposed by Sotgia et al. (2008), is that the transition is marked by a value of the so-called equivalent velocity that is independent of the pipe diameter (but instead only depends on the fluid properties). The equivalent velocity is defined as $\omega = \sqrt{\rho_m U_m^2/\Delta\rho}$. For the fluid properties considered by Sotgia et al. (which are somewhat comparable to those in the present study) the transitional value is $\omega_t = 2.3$ m/s. This means that (for given fluid properties) the existence of core-annular flow requires a sufficiently high mixture velocity (with sufficiently small density difference). Fig. 13 compares the present simulations with this criterion. Following Sotgia et al. the equivalent velocity is shown as function of the effective Reynolds number introduced by Arney et al. (1996): $Re_A = \frac{\rho_c D U_m}{\mu_w}\left[1 + \eta^4\left(\frac{\mu_w}{\mu_o} - 1\right)\right]$, $\rho_c = (1-\eta^2)\rho_w + \eta^2\rho_o$, with $\eta = \sqrt{1-\alpha_w}$. The figure shows that the simulated wall-touch line does not coincide with the $\omega_t = 2.3$ criterion. In particular for the low-diameter simulations ($D = 10.5$ mm) the simulations predict that stable core-annular flow is possible at low values of the equivalent velocity (i.e. below $\omega_t = 2.3$ m/s).

A second criterion, as mentioned by Bannwart (2001), is that core-annular flow requires that a significant amount of oil needs to be present, namely $\alpha_w < 0.5$. As shown in Fig. 14, this condition is indeed satisfied in the considered simulation conditions.

A third condition, as proposed by Bannwart (2001), says that the existence of core-annular flow requires that the interfacial tension between the oil and water is sufficiently high. Or more precisely: $E_o^* > 8$, in which the effective Eötvös number is defined as $E_o^* = \frac{\pi\Delta\rho g D^2}{4\sigma}\alpha_w$. For lower values stratified flow will be found. This criterion was not confirmed by the experiments of Sotgia et al. (2008). As shown in Fig. 15, also the present simulations for the larger pipe diameter of $D = 21$ mm do not satisfy the Eötvös criterion.

Based on the above it seems that the condition of oil reaching the

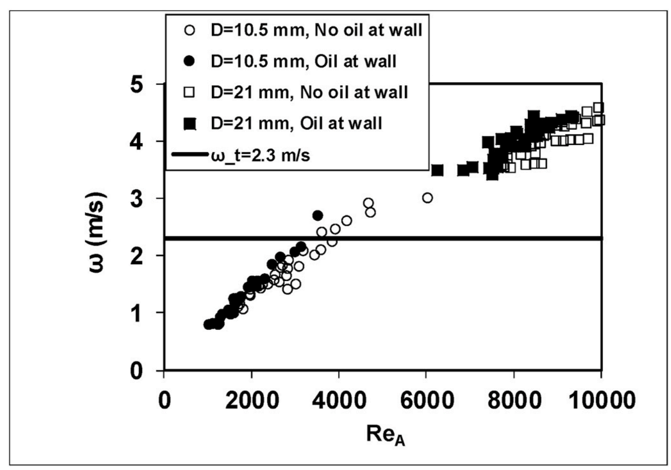

Fig. 13. Equivalent velocity as a function of the Arney formulation of the Reynolds number ($m = 1040$).

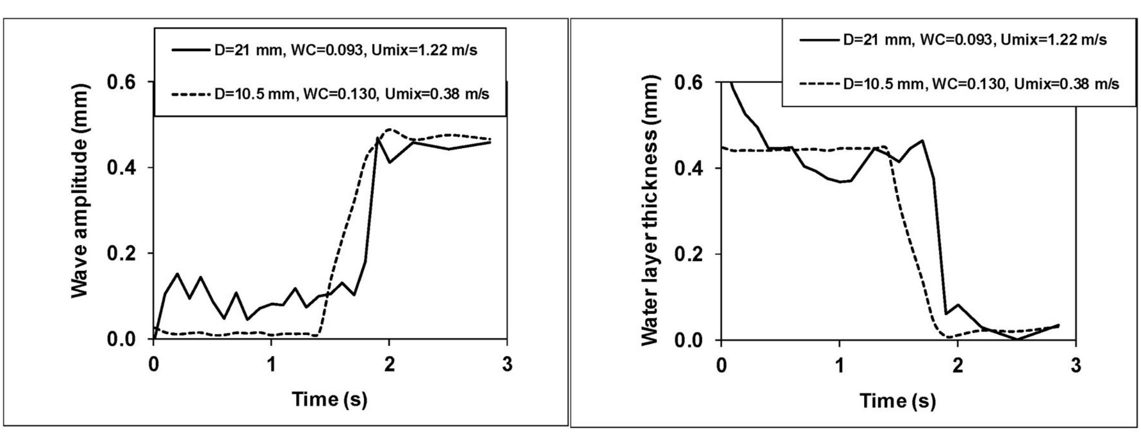

a) wave amplitude **b) water layer thickness**

Fig. 12. The effect of the pipe diameter on the amplitude and the water annulus at the top.

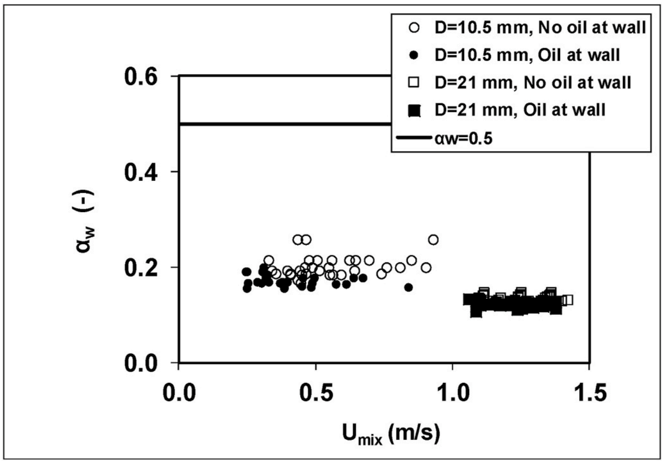

Fig. 14. The water holdup fraction in the considered cases ($m = 1040$).

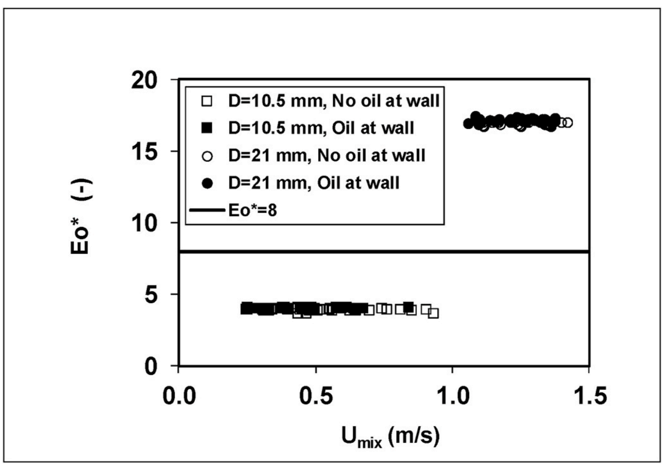

Fig. 15. The effective Eötvös number in the considered cases ($m = 1040$).

pipe wall in the present simulations is not related to the transition from core-annular flow to stratified flow.

5.2. Wave amplitude growth

For the simulation results shown in Fig. 11, the critical values of the watercut and of the mixture velocity are about those listed in Table 1 (for a viscosity ratio $m = 1040$). When fitted to the forms $\varepsilon_{w,crit} = C_1 D^q$ and $U_{mix,\ crit} = C_2 D^r$, filling in the values from Table 1 gives $q = -0.54$ and $r = 1.87$. Note that the value of q is close to -0.5, and the value of r is close to 2. Unfortunately these powers cannot directly be related to well-known dimensionless numbers (like the Reynolds number, the Froude number, or the Eötvös), which underpins again the complexity of the scaling of core-annular flow.

At least the simulations show that for the small pipe diameter ($D = 10.5$ mm) stable core-annular flow exists up to significantly lower values of the mixture velocity than for the larger pipe diameter ($D = 21$ mm). The simulations also show that stable core-annular flow can no longer

Table 1
Approximation of the predicted critical values for U_{mix} or the watercut for the onset of fouling (viscosity ratio is $m = 1040$).

D mm	$\varepsilon_{w,crit}$	$U_{mix,\ crit}$ m/s
10.5	0.14	0.3
21	0.096	1.1

exist if the watercut becomes too low. If there is insufficient water, the wave amplitude grows to a large value causing the wave to cross the thin water annulus and to touch the pipe wall.

The simulations in which oil reached the wall due to wave growth do not prove that core-annular flow without oil reaching the wall under the considered conditions is never possible. The occurrence of wall touching by the oil might be dependent on the way in which the dynamic simulations have been carried out. Here we started with perfect core-annular flow and allowed the waves to develop and the oil core to move upward. If the transient wave growth is too slow (e.g. due to the high viscosity of the oil) the levitation force resulting from the waves (meant to push the oil core off from the top wall) has not been timely established to stop the upward movement of the oil core. This means that the oil has already touched the top wall before stable core-annular flow could be established.

6. Conclusions

The occurrence and stability of core-annular flow in a horizontal pipe is complex and typically depends on 6 dimensionless numbers. Therefore, it is an ambitious task to try to simulate this. Nevertheless, we have tried to demonstrate what can obtained with respect to the flow dynamics of oil reaching the pipe wall using a state of the art numerical flow solver (the OpenFoam package with the CLSVOF solver for the RANS equations, applying the Launder-Sharma low-Reynolds number k-ε model for the turbulent water annulus). Each simulation did start with perfect core-annular flow (i.e. centred oil core without interfacial waves) and the wave formation and upward movement of the oil core was monitored over time. The wave growth either saturated at a finite value without touching the upper pipe wall or the wave did touch the upper wall.

The findings can be summarized as follows:

- The event in which the oil reaches the pipe wall (with imposed pressure drop) immediately leads to a sharp decrease in the flow rate (or mixture velocity).
- For each value of the pressure drop (or mixture velocity) there is a critical value of the watercut below which the oil will touch the pipe wall. This critical value of the watercut is lower for the larger pipe diameter of 21 mm, namely about 9.6%, than for the smaller pipe diameter of 10.5 mm, namely about 14% (for a viscosity ratio $m = 1040$).
- The oil also reaches the pipe wall when the mixture velocity is too low, but this lower limit is significantly higher for the larger pipe diameter of 21 mm, namely about 1.1 m/s, than for the smaller pipe diameter, namely about 0.3 m/s (for a viscosity ratio $m = 1040$).
- When the viscosity ratio is increased for the larger pipe diameter of 21 mm (starting at $m = 1040$), the critical watercut below which the oil reaches the pipe wall is found to decrease from about 9.6% to a minimum of about 7.2% at $m = 7500$. For even larger viscosity ratios the critical watercut slightly increases again.
- The occurrence of oil reaching the pipe wall in the CFD simulations cannot directly be related to well-known dimensionless numbers (like the Reynolds number, the Froude number, or the Eötvös). This underpins the complexity of the scaling of core-annular flow.
- The wall-touch lines derived from the present simulations do not confirm the relevance of all the criteria for the transition from core-annular flow to stratified flow that were proposed by Bannwart (2001) and Sotgia et al. (2008).
- As the event of oil reaching the pipe wall in the present simulations does not seem to be related to the transition to stratified flow, it is very well possible that the growing waves only temporarily or permanently touch the wall, while the core-annular flow is maintained. In actual reality for the latter condition, it depends on the adhesive properties between the oil and the pipe wall material whether the oil indeed remains stuck to the wall and fouls the pipe

wall. In the CFD simulations this adhesive behaviour is not modelled, and the simulation was stopped as soon as the oil touched the pipe wall.

- The CFD simulations in which the oil reaches the pipe wall due to wave growth do not prove that stable core-annular flow (i.e. the oil does not touch the pipe wall) under the considered conditions is never possible. Another choice of the initial conditions of the oil/water in the simulations might exist that does not give a temporary overshoot of the wave amplitude that gives wall touch. Additional simulations are needed to further investigate this.

Credit author statement

The first author has carried out the simulations. All authors have equally contributed to the definition of the cases and the interpretation of the results. The first and last author have been leading the writing of the paper.

Declaration of competing interest

The authors declare that they have no known competing financial interests or personal relationships that could have appeared to influence the work reported in this paper.

Acknowledgments

The authors gratefully acknowledge the research support from the Visiting Scholar Scholarship of the China Scholarship Council (CSC201809945004), the Natural Science Foundation of Guangdong Province (2016A030313653), and the Science and Technology Plan of Guangzhou City (201607010291).

References

Archibong-Eso, A., Shi, J., Baba, Y.D., Aliyu, A.M., Raji, Y.O., Yeung, H., 2019. High-viscous oil-water two-phase flow: experiments & numerical simulations. Heat Mass Tran. 55 (3), 755–767.

Arney, M.S., Ribeiro, G.S., Guevara, E., Bai, R., Joseph, D.D., 1996. Cement-lined pipes for water lubricated transport of heavy oil. Int. J. Multiphas. Flow 22 (2), 207–221.

Bannwart, A.C., 2001. Modelling aspects of oil–water core–annular flows. J. Petrol. Sci. Eng. 32 (2), 127–143.

Beerens, J.C., Ooms, G., Pourquié, M.J.B.M., 2014. A comparison between numerical predictions and theoretical and experimental results for laminar core-annular flow. AIChE J. 60, 3046–3056.

Ghosh, S., Mandal, T.K., Das, G., Das, P.K., 2009. Review of oil water core annular flow. Renew. Sustain. Energy Rev. 13, 1957–1965.

Ghosh, S., Das, G., Das, P.K., 2011. Simulation of core annular in return bends-A comprehensive CFD study. Chem. Eng. Res. Des. 89, 2244–2253.

Huang, A., Joseph, D.D., 1995. Stability of eccentric core-annular flow. J. Fluid Mech. 282, 233–245.

Ingen Housz, E.M.R.M., Ooms, G., Henkes, R.A.W.M., Pourquié, M.J.B.M., Kidess, A., Radhakrishnan, A.R., 2017. A comparison between numerical predictions and experimental results for horizontal core-annular flow with a turbulent annulus. Int. J. Multiphas. Flow 95, 217–282.

Jiang, F., Wang, Y., Ou, J., Xiao, Z., 2014. Numerical simulation on oil-water annular flow though the π bend. Ind. Eng. Chem. Res. 53, 8235–8244.

Jing, J., Sun, J., Tan, J., Huang, M., Liang, Q., Xue, T., 2016. Investigation on flow patterns and pressure drops of highly viscous crude oil-water flows in a horizontal pipe. Exp. Therm. Fluid Sci. 72, 88–96.

Joseph, D.D., Bai, R., Chen, K.P., Renardy, Y.Y., 1997. Core-annular flows. Annu. Rev. Fluid Mech. 29, 65–90.

Joseph, D.D., Bai, R., Mata, C., Sury, K., Grant, C., 1999. Self-lubricated transport of bitumen froth. J. Fluid Mech. 386, 127–148.

Kaushik, V.V.R., Ghosh, S., Das, G., Das, P.S., 2012. CFD simulation of core annular flow through sudden contraction and expansion. J. Petrol. Sci. Eng. 86–87, 153–164.

Kim, K., Choi, H., 2018. Direct numerical simulation of a turbulent core-annular flow with water-lubricated high viscosity oil in a vertical pipe. J. Fluid Mech. 849, 419–447.

McKibben, M.J., Gillies, R.G., Shook, C.A., 2000. A laboratory investigation of horizontal well heavy oil-water flows. Can. J. Chem. Eng. 78 (4), 743–751.

Oliemans, R.V.A., Ooms, G., 1986. Core-annular flow of oil and water through a pipeline. Multiphas. Sci. Technol. 2, 427–479.

Ooms, G., 1972. The hydrodynamic stability of core-annular flow of two ideal liquids. Applied Scientific Research Section A-Mechanics Heat Chemical Engineering Mathematical Methods, 26, pp. 147–158.

Ooms, G., Segal, A., Vanderwees, A.J., Meerhoff, R., Oliemans, R.V.A., 1984. A theoretical model for core-annular flow of a very viscous oil core and a water annulus through a horizontal pipe. Int. J. Multiphas. Flow 10, 41–60.

Ooms, G., Pourquié, M.J.B.M., Beerens, J.C., 2013. On the levitation force in horizontal core-annular flow with a large viscosity ratio and small density ratio. Phys. Fluids 25, 032102.

Radhakrishnan, R., 2016. Numerical Simulations and Experiments for Core-Annular Flow. Master of Science Thesis. Delft University of Technology.

Rodriguez, O.M.H., Bannwart, A.C., 2006. Experimental study on interfacial waves in vertical core-annular flow. J. Petrol. Sci. Eng. 54, 140–148.

Shi, J., Lao, L., Yeung, H., 2017a. Water-lubricated transport of high-viscosity oil in horizontal pipes: the water holdup and pressure gradient. Int. J. Multiphas. Flow 96, 70–85.

Shi, J., Yeung, H., 2017b. Characterization of liquid-liquid flows in horizontal pipes. AIChE J. 63 (3), 1132–1143.

Sotgia, G., Tartarini, P., Stalio, E., 2008. Experimental analysis of flow regimes and pressure drop reduction in oil-water mixtures. Int. J. Multiphas. Flow 34, 1161–1174.

Sridhar, S., Zhang, H.Q., Sarica, C., Pereyra, E.J., 2011. Experiments and model assessment on high-viscosity oil/water inclined pipe flows. In: SPE Annual Technical Conference and Exhibition, 2011, 30 October - 2 November.

Van Duin, H.J., 2017. Influence of Oil Viscosity on Oil-Water Core-Annular Flow through a Horizontal Pipe. Master of Science Thesis. Delft University of Technology.

Van Duin, Erik, Henkes, Ruud, Ooms, Gijs, 2019. Influence of oil viscosity on oil-water core-annular flow through a horizontal pipe. Petroleum 5 (2), 199–205.

Vuong, D.H., Zhang, H.Q., Sarica, C., Li, M., 2009. Experimental study on high viscosity oil/water flow in horizontal and vertical pipes. In: SPE Annual Technical Conference and Exhibition, 4–7 October. Louisiana, New Orleans.

Yamamoto, F., Okano, Y., Dost, S., 2017. Validation of the S-CLSVOF method with the density-scaled balanced continuum surface force model in multiphase systems coupled with thermocapillary flows. Int. J. Numer. Methods Fluid. 83, 223–244.